Automation of Biomarker Preconcentration, Capture, and Nanozyme Signal Enhancement on Paper-Based Devices

Daniel W. Bradbury,[†] Milad Azimi,[†] Alexia J. Diaz,[†] April A. Pan,[†] Cecilie H. Falktoft,[†] Benjamin M. Wu,[†,‡] and Daniel T. Kamei[†,*]

[†]Department of Bioengineering, University of California, Los Angeles, CA 90095

[‡]Division of Advanced Prosthodontics & Weintraub Center for Reconstructive Biotechnology, School of Dentistry, University of California, Los Angeles, CA 90095

ABSTRACT: Infectious diseases remain one of the leading causes of deaths in developing countries due to a lack of basic sanitation, healthcare clinics, and centralized laboratories. Paper-based rapid diagnostic tests, such as the lateral-flow immunoassay (LFA), provide a promising alternative to the traditional laboratory-based tests; however, they typically suffer from having a poor sensitivity. Biomarker preconcentration and signal enhancement are two common methods to improve the sensitivity of paper-based assays. While effective, these methods often require multiple liquid handling steps which are not ideal for use by untrained personnel in a point-of-care setting. Our lab previously discovered the phenomenon of aqueous two-phase system (ATPS) separation on paper which allowed for the seamless integration of concentration and detection of biomarkers on the LFA. In this work we have extended the functionality of ATPS separation on paper to automate the sequential delivery of signal enhancement reagents in addition to concentrating biomarkers. The timing of reagent delivery was controlled by changing the initial composition of the ATPS. We applied this technology to automate biomarker concentration and nanozyme signal enhancement on the LFA, resulting in a 30-fold improvement in detection limit over the conventional LFA when detecting *Escherichia coli*, all while maintaining a single-user application step

Infectious diseases are among the leading causes of deaths in developing countries. Many of these deaths could be prevented if the diseases were detected in their early stages, allowing for better patient management, faster administration of appropriate treatment, and more effective outbreak prevention.[1,2] However, the current gold standard diagnostic technologies capable of providing rapid and accurate detection are not suitable for use in developing countries which lack access to electricity, laboratory equipment, and trained personnel. The World Health Organization has provided the ASSURED criteria to aid in the development of point-of-care (POC) diagnostic tests specifically for use in developing countries. It states that such tests must be affordable, sensitive, specific, user-friendly, rapid and robust, equipment-free, and deliverable to the end-user.[1] Recently, paper has emerged as an excellent material for developing POC devices due to its low cost, ease of functionalization, and ability to passively transport fluid via capillary flow.[3] One common paper-based device is the lateral-flow immunoassay (LFA), a rapid antibody-based test that has achieved widespread commercial success in the form of the over-the-counter pregnancy test. Despite this success, the LFA does suffer from having a low sensitivity relative to laboratory-based tests, such as the enzyme-linked immunosorbent assay and the polymerase chain reaction, which limits its effectiveness in the detection of infectious diseases.[4]

To improve the sensitivity of the LFA, our group previously developed equipment-free methods which utilize liquid-liquid extraction techniques to concentrate the target biomarker prior to detection. This was achieved by using aqueous two-phase systems (ATPSs), which separate into two distinct phases, where the target biomarker would partition extremely into one of those phases, effectively concentrating it. The first method we developed required the ATPS to macroscopically separate, followed by the manual extraction of the phase containing the concentrated biomarker and then application to the LFA. While effective at improving the LFA detection limit by 10-fold for both large viruses[5,6] and small protein targets,[7,8] this approach was limited by its long time-to-result and requirement of multiple user-steps. To address these limitations, a second method was developed which involved the direct application of a mixed ATPS to a paper device. Our lab discovered that a well-mixed ATPS rapidly separated into its macroscopic phases as it flowed through a paper membrane, producing distinct leading and lagging phases. Integration of this ATPS separation on paper phenomenon with the LFA allowed for simultaneous analyte concentration and detection, while reducing the overall time-to-result.[9,10]

In addition to biomarker preconcentration, another equipment-free method to improve the sensitivity of the LFA involves chemical signal enhancement. Chemical signal enhancement typically requires the user to manually apply enhancement reagents to the LFA test strip in a sequential manner. Although these methods are effective at improving LFA sensitivity, the requirement of multiple user steps renders them not ideal for a POC device.[11,12] To eliminate the need for multiple user steps, the Yager group developed 2D paper networks, which utilize carefully designed 2D paper geometries to control fluid flow and perform timed delivery of reagents to a detection zone.[13–16] Other paper-based automation techniques include the use of controlled porosity,[17] paper shunts,[18] valves,[19–22] and dissolvable sugar delays.[23,24] While successful at automating enhancement reactions, many of the devices using these techniques have

thus far demonstrated limited improvements in detection limit over their unenhanced counterparts. Additionally, many of these devices are significantly more complex than the conventional LFA test strip, which could increase cost and limit their adaptability for high volume manufacturing.[25]

In this work, we introduce a new technique to automate both biomarker concentration and signal enhancement which is easy to use, low in cost, tunable without complex changes in device design, and easily manufacturable. We have called this technique the **A**TPS-automated **C**oncentration and **E**nhancement of the **L**ateral-**F**low immuno**A**ssay (ACE-LFA). The ACE-LFA takes advantage of both the selective partitioning of biomarkers and reagent molecules between the phases of the ATPS, as well as our lab's ATPS separation on paper technology to sequentially deliver the concentrated target biomarker and signal enhancement reagents across the LFA test strip. We demonstrated that the delivery time of reagents is tunable by simply changing the initial composition of the ATPS. In a proof-of-concept demonstration, we used our ACE-LFA technology to automate the preconcentration and capture of the model bacteria *Escherichia coli* (*E. coli*) along with a nanozyme signal enhancement reaction, which ultimately resulted in a 30-fold improvement in detection limit over the conventional LFA. To our knowledge, this is the first reported use of the ATPS to automate sequential reagent delivery, as well as the first integration of automated biomarker concentration, capture, and signal enhancement on a paper-based device.

MATERIALS AND METHODS

Preparation and characterization of ATPSs for flow studies. All reagents and materials were purchased from Sigma-Aldrich (St. Louis, MO) unless noted otherwise. Poly(ethylene glycol-*ran*-propylene glycol) (12 kDa) (EOPO) and sodium citrate salt (2.6:1 trisodium citrate:citric acid to maintain pH 5) were dissolved in diH_2O. Three different ATPSs with 3:1 equilibrium volume ratios (volume of the top phase divided by the volume of the bottom phase) were found by varying the initial % w/w compositions of EOPO and salt. For individual phase characterization, 10 g ATPSs were made. Each solution was vortexed and allowed to phase separate overnight. After phase separation was completed, the solution was centrifuged for 5 min at 2000 rpm, and the immiscible phases were extracted using a pipette and collected in separate tubes for characterization. The viscosity of each phase was measured in triplicate using a Brookfield LVDV-I Prime digital viscometer (AMETEK Brookfield, MA). The surface tension of each phase was measured using a Krüss K6 force tensiometer (Krüss USA, NC). For the flow studies, 0.5 g ATPSs were made with 5 μL of brilliant blue FCF dye to aid in visualization of the phases. A detailed breakdown of ATPS component quantities for the flow studies and ACE-LFA studies can be found in Table S1 (ESI).

Demonstration of automated and tunable reagent delivery on paper using ATPSs. Flow studies were conducted to measure the speeds of ATPS phases as they separated and flowed through fiberglass paper via capillary action. The fiberglass paper was mounted onto an adhesive backing and cut into 3 mm × 67 mm strips. A three-dimensional (3D) paper wick was placed at the lower end of the strip which aided in the separation of the ATPS as it flowed through the paper. This wick was composed of five stacked sheets of 7 mm x 15 mm fiberglass paper. The paper setup was enclosed in a custom-made acrylic cassette to hold the wick together and minimize effects of evaporation. The top piece of the acrylic cassette was marked every 5 mm along the length of the strip. To run the flow studies, the wick end of the paper setup was dipped into a 24 well plate containing a 0.5 g well-mixed ATPS with blue dye (Fig. 1A). The wicking process was recorded using a Nikon D3400 digital camera (Nikon, Tokyo, Japan). Experiments were performed in triplicate and analyzed using QuickTime Player (Apple, Cupertino, CA) to track the locations of each phase as they flowed through the paper setup.

Preparation of bacteria cell cultures. *Escherichia coli* O157:H7 (*E. coli)* (ATCC® 700728™) were cultured according to manufacturer protocol (ATCC, Manassas, VA) and plated onto Difco Nutrient Agar (Becton, Dickson and Company, Sparks, MD) plates. The plated cells were incubated at 37ºC aerobically overnight and then the plate was sealed with Parafilm and stored at 4ºC until use. To prepare liquid bacterial cultures, single colonies were picked from the agar plate and cultured in 5 mL of Difco Nutrient Broth (Becton, Dickson and Company, Sparks, MD). The cells were incubated at 37ºC and 250 rpm on a shaking incubator for 16 h. To quantify the bacteria concentrations within the original liquid suspension, serial dilutions of bacteria were plated and colonies were counted after overnight incubation.

Measuring the partitioning of *E. coli* and TMB in ATPS. To measure the partitioning of both *E. coli* and 3,3',5,5'-tetramethylbenzidine (TMB) in the EOPO-salt ATPS, either ~10^7 cells or 10 μL of an 816 mM TMB solution in dimethylformamide (DMF) were added to an ATPS with a total final mass of 0.5 g. The ATPSs were vortexed and allowed to phase separate at room temperature (22°C) for 2 h. Each phase of the ATPS was carefully withdrawn using a micropipette and diluted in water. For the *E. coli* partitioning studies, the EOPO-rich top phase and EOPO-poor bottom phases were diluted by 2-fold. A hemocytometer (Thermo Fisher Scientific, Waltham, MA) was used to count the total number of cell entities in each phase. The partition coefficient for *E. coli*, which is defined as the concentration of *E. coli* in the top phase divided by the concentration in the bottom, was then calculated. The hemocytometer was used in these experiments instead of counting colonies to avoid possible error caused by the ATPS components inhibiting bacteria growth. For the TMB partitioning studies, the EOPO-rich top phase was diluted by 100-fold, while the EOPO-poor bottom phase was diluted by 10-fold to reduce interference caused by the phase forming components during analysis. The absorbance at the peak wavelength for reduced TMB ($\lambda_{max} = 286$ nm) was then measured for each diluted phase using a GENESYS 10S UV-Vis spectrophotometer (Thermo Fisher Scientific, Waltham, MA). The partition coefficient for TMB was calculated by multiplying the measured absorbances by the dilution factor and then taking the ratio of the resulting values for the top and bottom phases. Each partitioning experiment was performed in triplicate.

Preparation of antibody-decorated nanozyme and nanoparticle probes. Platinum-coated gold nanozymes (PtGNs) were synthesized using a protocol derived from Gao *et. al.* which is described in the ESI.[26] To create anti-*E. coli* platinum-coated gold nanozyme probes (PtGNPs), 20 μL of a 0.1 M sodium borate solution (pH 9) was first added to 1 mL of PtGNs. Then, 4 μg of primary Bactrace anti-*E. coli* O157:H7 antibody (Seracare, Milford MA) was added to the suspension and incubated for 30 min at room temperature (22°C). 50 μL of a 10% (w/v) bovine serum albumin (BSA) solution was then added to

the suspension and incubated for 10 min. Free antibodies were removed by centrifugation and the pellet was resuspended in 50 μL of a 0.1 M sodium borate (pH 9) solution. Anti-*E. coli* gold nanoprobes (GNPs) were made using the same procedure; however, 40 nm GNs were used in place of PtGNs at the same concentration.

Detection of *E. coli* using the conventional LFA. The conventional LFA strips were composed of overlapping pads secured to an adhesive backing. These pads included a sample pad, a conjugate pad, a nitrocellulose membrane, and a CF6 absorbent pad (GE Healthcare Bio-Sciences, Pittsburgh, PA). In our work, the sample pad consisted of a 3 mm × 10 mm Standard 17 fiberglass paper (GE Healthcare Bio-Sciences) treated with a running buffer (0.4% BSA, 0.6% Tween 20, and 0.2% polyethylene glycol in phosphate-buffered saline, pH 7.4). GNPs were dehydrated onto a 3 mm x 10 mm fiberglass paper along with a 1% BSA in diH_2O solution to form the conjugate pad. Both the sample and conjugate pads were dehydrated under very low pressure using a Labconco FreezeZone 4.5 lyophilizer (Thermo Fisher Scientific, Waltham, MA) for 2 h. LFA strips in this study utilized the sandwich assay format where Bactrace anti-*E. coli* antibody were immobilized on a Unistart CN95 nitrocellulose membrane (Sartorius, Göttingen, Germany) at 0.5 mg/mL. This constituted the test line of the test strip. Anti-goat antibodies (Bethyl, Montgomery, TX) were immobilized at 0.25 mg/mL to constitute the control line of the test strip. Test and control line printing was performed by dispensing 50 μL of antibody solution per 30 cm of nitrocellulose membrane using an Automated Lateral Flow Reagent Dispenser (Claremont BioSolutions, Upland, CA) and a Fusion 200 syringe pump (Chemyx, Stafford, TX) with a flow rate of 300 μL/min. The membrane was left in a vacuum-sealed desiccation chamber overnight. The nitrocellulose membrane was placed on the adhesive backing and cut into strips 3 mm in width prior to assembly with the sample pad, conjugate pad, and absorbent pad. The LFA test strip was placed in a custom-made acrylic cassette to limit evaporation while running the assay. The top of the cassette also applied light pressure to the conjugate pad, aiding in the uniform flow through the conjugate pad and uniform release of the dehydrated GNPs.

To detect for *E. coli* in buffer using the conventional LFA, the test strip was inserted vertically into 125 μL of a sample suspension containing a known concentration of *E. coli* in phosphate-buffered saline (PBS). To detect for *E.* coli in Surine™ Negative Urine Control (Cerilliant, Round Rock, TX), the test strip was inserted into 165 μL of *E. coli* in Surine. Videos of the test strips were taken using a Nikon D3400 digital camera (Nikon, Tokyo, Japan). Additionally, photos were taken after 30 min in a controlled lighting environment. To quantify the test line intensities, images of the LFA test strips, as well as the video frames (1 frame per 3 min), were processed using a custom MATLAB script developed by our lab.[6]

Detection of *E. coli* using the ACE-LFA. The ACE-LFA setup was composed of a test strip as well as an ATPS solution with signal enhancement reagents. For the test strip, the conventional LFA strip design was modified to include a 3D paper wick instead of the sample pad. This wick was composed of five stacked sheets of 7 mm × 15 mm fiberglass paper with the top corners cut at a 45º angle (Fig. S1, ESI). PtGNPs were dehydrated onto the conjugate pad in place of the GNPs. The ACE-LFA test strip was enclosed in a custom-made acrylic cassette to hold the wick together and to limit evaporation while running the assay.

To detect *E. coli* in PBS using the ACE-LFA, a 0.5 g well-mixed 12.9% EOPO – 10% salt 3:1 volume ratio ATPS containing 10 μL of an 816 mM TMB solution in DMF, 10 μL of a 30% w/v hydrogen peroxide solution, 50 μL of a TMB stabilizing solution (Vector Laboratories, Burlingame, CA), and 5 μL *of E. coli* in PBS were added into a well of a 24 well plate. The 3D wick-modified test strip was then placed into the mixed ATPS, and the solution was allowed to pass through the wick towards the absorbent pad. To detect *E. coli* with the LFA + ATPS, the above ACE-LFA procedure was modified by replacing the TMB with 10 μL of DMF. To detect *E. coli* in Surine™ using the ACE-LFA, a 0.5 g well-mixed 12.9% EOPO – 8.2% salt ATPS containing 15 μL of an 816 mM TMB solution in DMF, 10 μL of a 30% w/v hydrogen peroxide solution, 100 μL of a TMB stabilizing solution, and 165 μL of *E. coli* in Surine™ were added into a well of a 24 well plate followed by the addition of the test strip.

Videos of the test strips were taken to monitor the signal development over time. Images of the resulting test strips were also taken after 30 min in a controlled lighting environment. To quantify the test line intensities, the video frames (1 frame per 3 min) and images were processed using a custom MATLAB script developed by our lab.

RESULTS AND DISCUSSION

Demonstration of tunable flow behavior and reagent delivery on paper using ATPSs. In this work, we hypothesized that the separation and flow of an ATPS through a paper membrane can be used to automate both biomarker preconcentration and the delivery of signal enhancement reagents on a paper-based device. Many varieties of ATPS exist; however, here we will be discussing the use of a polymer-salt system composed of EOPO and citrate salt. When salt is added to an aqueous solution of EOPO, the salt will disrupt the hydrogen bonds between the water and the oxygen atoms of the EOPO polymer chains. This will decrease the EOPO-water interactions and increase the EOPO-EOPO interactions, ultimately leading to phase separation where immiscible microscopic EOPO-rich and salt-rich (EOPO-poor) domains are formed to minimize the Gibbs free energy of the system.

To utilize this ATPS to sequentially deliver reagents as they flow through a paper device, the reagents to be delivered are first added to the mixed ATPS where they must partition or localize extremely into microdomains of the opposite phases. Subsequently, the ATPS is applied to a paper device where it will rapidly separate into its two bulk, macroscopic phases as it flows via capillary action. The reagents localized in the leading EOPO-poor phase of the ATPS will be delivered first to the region of interest on the paper device. This is then followed by the lagging EOPO-rich phase, which will deliver the reagents localized in that phase in an automated fashion. Note that, in this work, the "extreme" localization of reactive reagents into opposite macroscopic phases, means that the reagents are separated from one another to a great enough degree to prevent premature interactions that could result in undesired visible signal development.

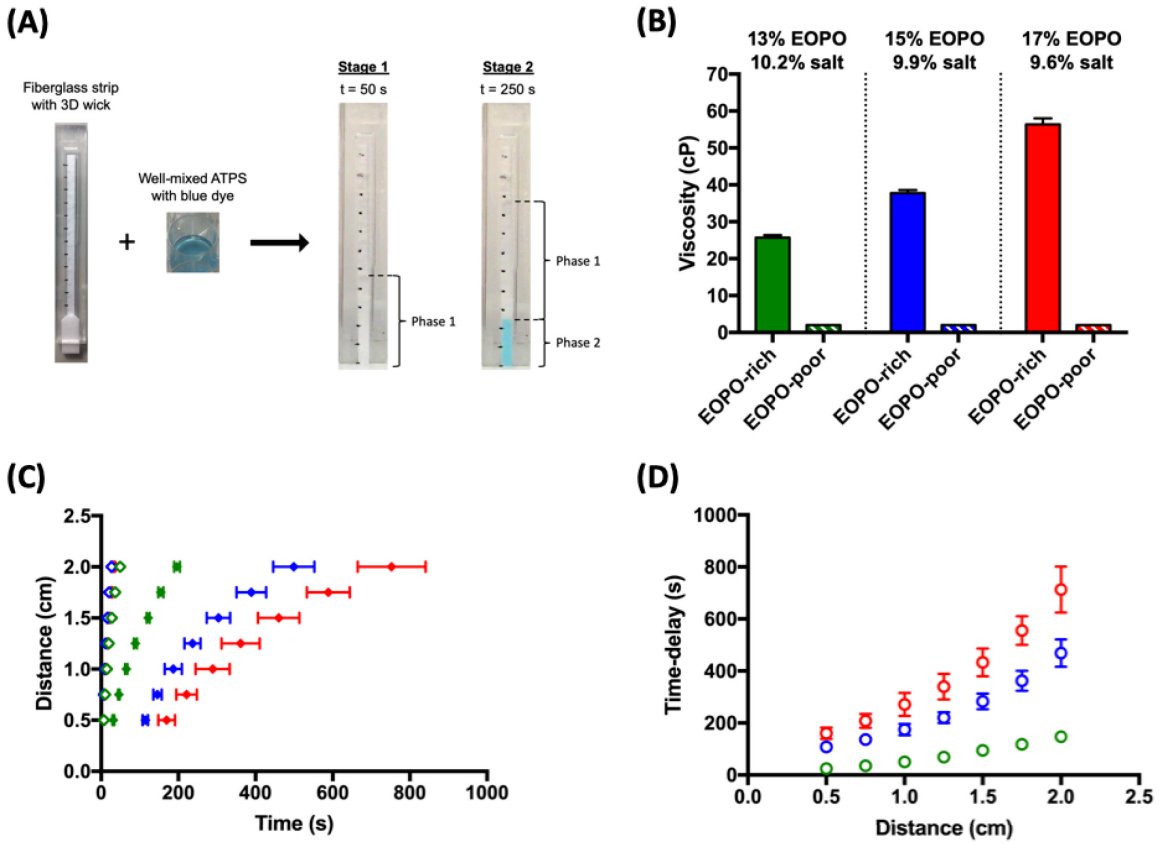

Figure 1. Flow studies. Green corresponds to the 13% EOPO – 10.2% salt ATPS, blue to the 15% EOPO – 9.9% salt ATPS, and red to the 17% EOPO – 9.6% salt ATPS. (A) Experimental setup for ATPS flow studies. (B) Viscosity measurements for the extracted ATPS phases. (C) Distance traveled up the paper strip by the air - phase 1 interface (◇,◇,◇) and the phase 1 - phase 2 interface (◆,◆,◆) as a function of time. (D) Time-delay between when the air - phase 1 interface and the phase 1 - phase 2 interface reach a particular distance on the paper strip (○,○,○). All of the data are presented as mean ± SD (n = 3).

When designing a system to automate reagent delivery, it is important to have tunable fluidic control. We hypothesized that we could achieve this fluidic control by changing the equilibrium state of the ATPS. By altering the initial concentrations of the phase forming components added to the ATPS, the properties such as the equilibrium volume ratio and concentrations of phase forming components in the equilibrium phases, can be changed, which will affect the physical properties that dictate flow behavior. For a polymer-salt ATPS system (such as the EOPO-salt system used in this study) with a fixed volume ratio, an increase in the initial concentration of polymer results in an increase in the concentration of polymer in the polymer-rich phase and a decrease in the concentration of polymer in the polymer-poor phase at equilibrium.[27] We anticipated that this increase in the equilibrium concentration of polymer in the polymer-rich phase would result in an increase in the viscosity of that phase, which in turn, would result in slower flow and a greater reagent delivery time. To confirm this, we experimentally found three different EOPO-salt ATPS compositions that yielded a 3:1 volume ratio. The measured viscosities of the EOPO-rich and EOPO-poor phases for these systems are shown in Fig. 1B. Consistent with our expectations, as the concentration of EOPO initially added to the ATPS increased, the viscosity of the EOPO-rich phase also increased from 25.7 ± 0.7 cP for the 13% EOPO – 10.2% salt ATPS to 37.8 ± 0.8 cP for the 15% EOPO – 9.9% salt ATPS to 56.4 ± 1.6 cP for the 17% EOPO – 9.6% salt ATPS. The viscosities of the EOPO-poor phases were found to be constant for all systems tested.

For each different ATPS, the locations of the air - EOPO-poor phase (air - phase 1) interface and the EOPO-poor phase - EOPO-rich phase (phase 1 - phase 2) interface were tracked and plotted versus time (Fig. 1C). It is observed that an increase in the initial concentration of EOPO in the ATPS resulted in a slower moving phase 1 - phase 2 interface. This was expected because increasing the initial EOPO concentration made the EOPO-rich phase more viscous, and higher viscosity leads to slower flow. We next calculated the time delay between when the air - phase 1 interface and the phase 1 - phase 2 interface reached the same distance along the paper strip. The time delay is an important metric to be able to control when designing automated reactions and assays, because different applications may require shorter or longer durations of time between the delivery of the reagents. It was observed that the time delay increased with an increase in both the viscosity of the EOPO-rich phase and the distance along the strip. These trends were expected as it is well-established that the viscous resistance, which acts to slow fluid flow, increases with an increase in viscosity and/or an increase in length of the fluid segment.[28] Time delays ranging from 30 to 840 s were achieved in our experiments. Note that greater delays may be obtained by choosing different ATPS systems with phases that have higher viscosities, such as a polymer-polymer or micellar ATPS.

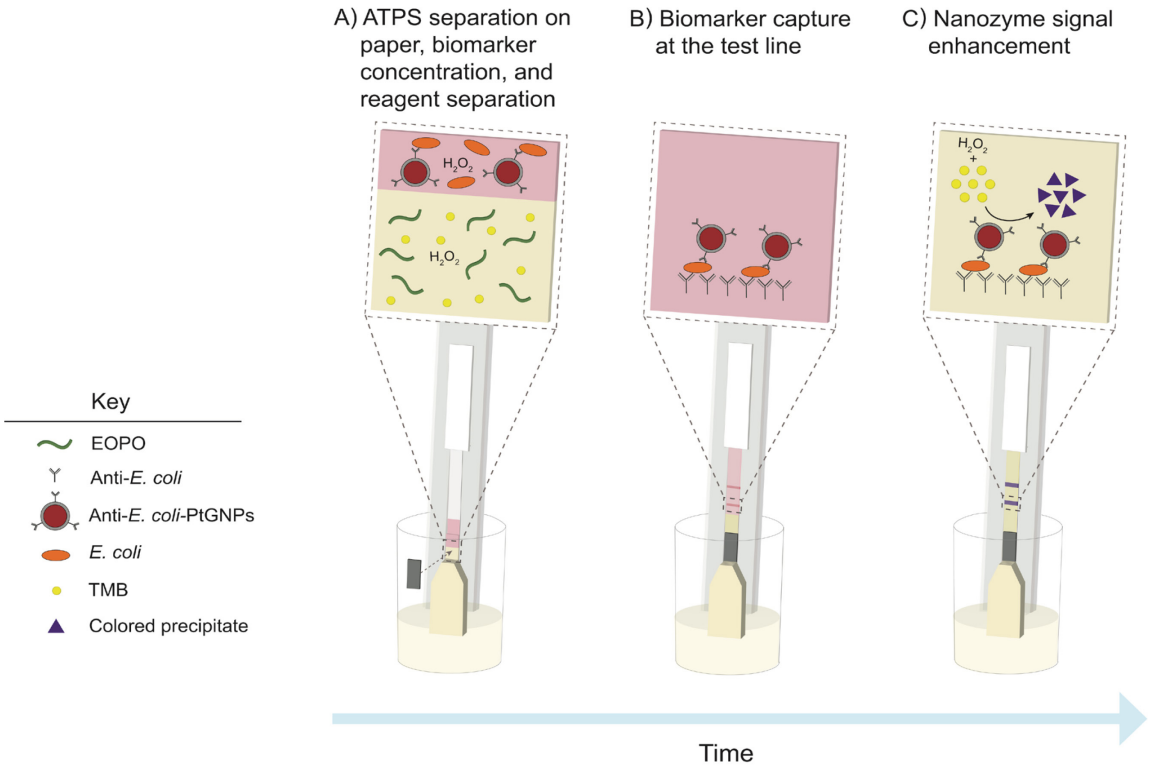

Figure 2. Schematic of ACE-LFA for the detection of *E. coli*. (A) The test strip is dipped into an ATPS solution which phase separates as it flows through the paper. *E. coli* is concentrated in the leading phase, and the TMB partitions preferentially into the lagging phase. The leading phase delivers the concentrated *E. coli* and rehydrated PtGNPs to the detection zone. (B) Biomarker capture occurs at the LFA detection zone where *E. coli* is sandwiched between the test line antibodies and the PtGNPs. (C) This is followed by the lagging phase, which delivers the TMB substrate to initiate the nanozyme signal enhancement reaction.

Demonstration of improved detection limit using ACE-LFA with nanozymes. After demonstrating the tunable nature of ATPS flow on paper, we next sought to apply this technology to automate a nanozyme-based signal enhancement reaction, and to concentrate and detect *E. coli* on an LFA test. We have called this new technology the **A**TPS-automated **C**oncentration and **E**nhancement of the **L**ateral-**F**low immuno**A**ssay (ACE-LFA). A nanozyme-based signal enhancement reaction was chosen due to its high catalytic activity and stability when compared to the more traditional enzyme-catalyzed reactions. More specifically we have utilized a recently developed nanozyme system containing platinum-coated gold nanozymes which catalyze the oxidation of TMB in the presence of hydrogen peroxide to produce a dark precipitate.[26] To run the ACE-LFA, a test strip with a 3D wick was dipped into an ATPS containing *E. coli* and the signal enhancement reagents: TMB, hydrogen peroxide, and TMB stabilizing solution. We initially chose the 13% EOPO – 10.2% salt ATPS for use in the ACE-LFA, because it was found to allow ~7 minutes for antibody binding before the lagging phase crossed the test line. This is comparable to many commercial assays and should allow reasonable time for antibody-antigen binding to occur at the test line as well as signal enhancement reagents to be delivered. When the signal enhancement reagents were added to the 13% EOPO – 10.2% salt ATPS, the observed volume ratio shifted from 3:1 to ~2:1. While this volume ratio shift is not completely understood, the proprietary TMB stabilizing solution, which is required to produce an insoluble rather than a soluble TMB product, was found to be responsible and thus must contain some compound that influences phase separation (i.e., salt, polymer, or organic solvent). Therefore, for the ACE-LFA demonstrations in this work, a 12.9% EOPO – 10% salt ATPS with the TMB stabilizer was used instead, which was found to produce a 3:1 volume ratio in a microcentrifuge tube and also had comparable flow behaviors to 13% EOPO – 10% salt ATPS without the stabilizer (data not shown).

Recall that reagents must be localized in opposite phases of the ATPS in order for them to be sequentially delivered. The partitioning of different molecules and particles between the two phases of an ATPS depends on a variety of physical and chemical properties, such as size, hydrophobicity, and electrochemical properties of the target species.[27] Due to its large size and hydrophilicity, the *E. coli* bacteria was expected to partition extremely into the EOPO-poor phase of the EOPO-salt ATPS, where it would experience fewer unfavorable, steric, excluded-volume interactions with the less abundant EOPO molecules in that phase. In the case of the 3:1 volume ratio used in this work, the *E. coli* would be forced into one-fourth of the original ATPS volume, thus concentrating it by four-fold. The TMB substrate, which is small and relatively hydrophobic, was expected to partition preferentially into the more hydrophobic EOPO-rich phase. The partition coefficients for both *E. coli* and TMB in our ATPS were measured to be 0.0029 ± 0.0005 and 11.1 ± 0.3, respectively. A partition coefficient value less than one indicates preferential partitioning to the EOPO-poor phase, and a value greater than one indicates preferential partitioning to the EOPO-rich phase. These results were consistent with our hypothesis that the *E. coli* and TMB would selectively localize into opposite ATPS phases.

When the ATPS containing *E. coli* and the signal enhancement reagents is added to the ACE-LFA test strip, it flows through the 3D wick and separates into its two macroscopic phases. First, the leading, EOPO-poor phase containing the concentrated *E. coli* bacteria solubilizes the dehydrated PtGNPs and delivers them to the LFA detection zone. Here, the presence of the target biomarker *E. coli* in sufficient quantities produces a visible pink or red test line, as the PtGNPs first bind to the *E. coli* and then these PtGNP - *E. coli* complexes become captured by the immobilized antibodies at the test line. An absence or insufficient quantity of *E. coli* results in no visible test line. Regardless of the presence or absence of *E. coli*, the control line appears, indicating that the PtGNPs flowed up the entire strip and that the test is therefore valid (Fig. 2). This is followed by the lagging, EOPO-rich phase, which delivers the TMB to the LFA detection zone. In the presence of hydrogen peroxide, TMB that comes into contact with the PtGNPs bound to the test and control lines will be converted into a dark purple precipitate, thereby enhancing the signal. It is important to note that because the TMB partitions favorably into the EOPO-rich phase, while the PtGNPs are rehydrated into the EOPO-poor phase, the reactive reagents are effectively separated from one another. It is this thermodynamic separation of reactive reagents within the ATPS, along with the ability of the ATPS to phase separate as it flows through paper, that allows for the automation of signal enhancement while avoiding premature signal development.

To demonstrate that the above process does indeed occur *and* to examine the ability of the ACE-LFA to automate the signal enhancement reaction and therefore improve signal over the conventional LFA, we tested each assay with an overall *E. coli* concentration of 10^6 colony forming units (cfu)/mL in the sample/ATPS. A video of the signal development was taken over the course of 30 min (ESI). For the conventional LFA, a visible pink test line developed within 15 min (Fig. 3). For the ACE-LFA, a pink test line was visible within the first 6 min of the assay. The earlier formation of the pink test line in the ACE-LFA compared to the conventional LFA was due to the *E. coli* being concentrated in the leading phase of the ATPS which only occurred in the ACE-LFA. For the ACE-LFA, the interface between the leading and lagging phase can be observed in the 6 min photo. After ~7 min, the lagging phase crossed the test line region, delivering the TMB and initiating the nanozyme signal enhancement reaction. (This can be observed in our signal development video, ESI). Signal enhancement was observed as the test and control line color changed from pink to purple. We also quantified the test line intensities using a MATLAB script developed by our lab and the results are plotted in Fig. S2. After 30 min of assay time, the test line intensity of the ACE-LFA was measured to be 14-fold greater than that of the conventional LFA (relative test line signal of ACE-LFA was 100.0 ± 7.9% compared to the conventional LFA at 7.0 ± 0.7%). These results confirmed that our ACE-LFA technology has the ability to successfully automate both biomarker preconcentration and nanozyme signal enhancement while maintaining a low background signal, suggesting that it may serve as a more sensitive alternative to the conventional LFA.

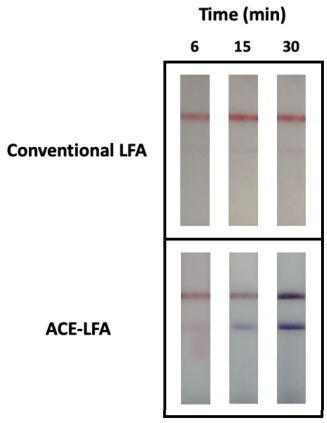

Figure 3. Comparing signal development over time for the conventional LFA and the ACE-LFA tested with 10^6 cfu/mL of *E. coli*.

We next wanted to determine if the ACE-LFA had an improved detection limit relative to the conventional LFA. First, we identified the detection limit of the conventional LFA with GNPs by testing dilutions of *E. coli* in PBS. The conventional LFA was able to successfully detect *E. coli* down to a concentration of 10^6 cfu/mL within 30 min, indicated by the formation

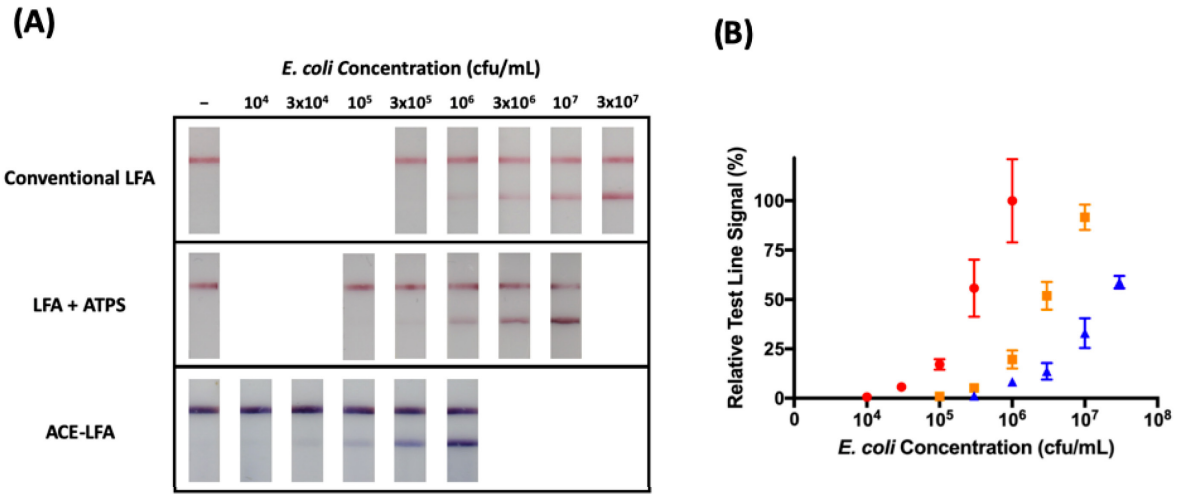

Figure 4. 30-fold improvement in detection limit when using ACE-LFA over the conventional LFA. (A) Conventional LFA detects down to 10^6 cfu/mL, LFA + ATPS detects down to 3.3×10^5 cfu/mL, and the ACE-LFA detects down to 3.3×10^4 cfu/mL of *E. coli* overall. (B) Plot of quantified relative test line signals vs. *E. coli* concentration for the conventional LFA (▲), LFA + ATPS (■) and ACE-LFA (●). All of the data are presented as mean ± SD (n = 3).

of 2 visible lines. On the other hand, the ACE-LFA was able to detect *E. coli* at 3.3×10^4 cfu/mL, demonstrating a 30-fold improvement in detection limit over the conventional LFA (Fig. 4A). This is also supported by the quantitative results shown in Fig. 4B, where the relative test line intensities for the conventional LFA at 10^6 cfu/mL and the ACE-LFA $3.3x10^4$ cfu/mL are comparable and the two curves are continuously separated by at least a 30-fold difference in the overall concentration of *E. coli* for approximately the same test line signal. We also found the detection limit of the LFA + ATPS (without the nanozyme-TMB enhancement) to be 3.3×10^5 cfu/mL, demonstrating a 3-fold improvement over the conventional LFA. This is similar to the expected 4-fold improvement in detection limit that would be due to the *E. coli* bacteria being effectively concentrated into the leading phase of the ATPS. This suggests that the nanozyme-TMB enhancement reaction alone was responsible for a 10-fold improvement in the LFA detection limit. Additionally, we compared the detection limit of the conventional LFA using GNPs versus PtGNPs and found that both assays have a detection limit of 10^6 cfu/mL of *E. coli* (Fig. S3, ESI), confirming that the 30-fold improvement in detection limit obtained from the ACE-LFA is a result of improvements from both biomarker preconcentration via the ATPS and signal enhancement via the ATPS-automated nanozyme reaction, and not any characteristic differences in the optical properties of the nanoprobes.

In these experiments, we demonstrated that the ACE-LFA can achieve a 30-fold improvement in detection limit over the conventional LFA if the overall concentration of *E. coli* was the same between the ATPS of the ACE-LFA and the sample added to the conventional LFA. This comparison is suitable for a swab-based test where a swab must be agitated in an excess of a predetermined buffer to release and dilute the sample prior to application onto a test strip. Using this type of setup, a swab could be agitated in the ATPS of the ACE-LFA ATPS or a buffer of the same volume for the conventional LFA, thus resulting in a similar concentration of *E. coli* in both solutions. Additionally, while the above conventional LFA detection panels were performed with a 4-fold lower volume than the ACE-LFA (125 µL vs. 500 µL), increasing the conventional LFA sample volume to 500 µL did not improve the detection limit (Fig S4, ESI). This is most likely because the solution was too large for all of the *E. coli* in the sample to interact with all of the rehydrated PtGNPs and completely flow past the test line, a common LFA problem. Therefore, one of the benefits of sample concentration techniques is that the biomarker present in a larger volume could be concentrated into a smaller volume where all of the biomarker could effectively interact with the PtGNPs and flow past the test line.

Finally, we evaluated the applicability of the ACE-LFA for detecting *E. coli* in a physiologically relevant liquid sample. *E. coli* was suspended in Surine™ Negative Urine Control, which is a Certified Reference Material for applications in clinical and analytical chemistry. For the conventional LFA, a 165 µL sample of *E. coli* in Surine™ was applied directly to the test strip. *E. coli* was successfully detected down to a concentration of 10^6 cfu/mL within 30 min (Fig. 5). In the case of the ACE-LFA, the 165 µL *E. coli* sample was added to the ATPS phase forming components and enhancement reagents resulting in an approximate 3-fold dilution in the ATPS. The ACE-LFA was able to detect down to 10^5 cfu/mL of *E. coli* in the original Surine™ sample (also corresponding to 3.3×10^4 cfu/mL overall in the ATPS), demonstrating a 10-fold improvement in detection limit from the point of view of the original *E. coli* sample. This is expected because the sample was first diluted 3-fold in the ATPS prior to being reconcentrated in the leading phase. This dilution reduced the observed fold improvement in detection limit from the previous 30-fold to 10-fold. Ultimately, even with this dilution and using a more complex sample, we've demonstrated that the ACE-LFA can achieve a significant improvement in detection limit over the conventional LFA.

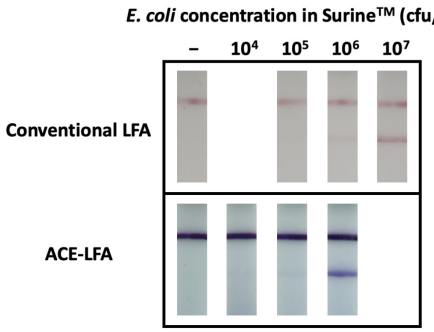

Figure 5. 10-fold improvement in detection limit for *E. coli* in Surine™. Conventional LFA detects down to 10^6 cfu/mL while ACE-LFA detects down to 10^5 cfu/mL of *E. coli* in Surine™.

The importance of developing new methods of fluidic control for paper-based devices that require minimal user intervention and are compatible with high volume manufacturing was recently highlighted by Fu and Downs.[25] We believe that the ACE-LFA technology developed here is a significant contribution to addressing this need with several potential benefits over the previously developed automation techniques. For one, unlike many of the previous techniques, the device footprint of our ACE-LFA is very similar to the conventional LFA and it does not require complex paper geometries or electronic actuators. As a result, the ACE-LFA should be compatible with currently available high-volume LFA manufacturing techniques and will thus retain a low cost. Secondly, the ACE-LFA also has the potential to achieve higher levels of improvement over other techniques, because it can integrate both biomarker concentration and signal enhancement into a single device. This can be useful for the detection of biowarfare agents, infectious diseases, and food-borne illnesses, where it is desirable to detect the target at the lowest possible concentration.

The ACE-LFA procedure used in this work, which required an initial mixing step prior to the addition of the ATPS onto the test strip, is well suited for applications that require initial mixing into a predetermined buffer (i.e., swab-based diagnostics). However, other diagnostic applications may benefit from the direct application of a sample to the test without any mixing or sample dilution steps. To address this, our lab has recently demonstrated that ATPS components can be dehydrated on paper and then rehydrated upon addition of a sample fluid to induce phase separation and biomarker preconcentration without the need for any user mixing steps.[29] Future work will therefore aim to dehydrate the signal enhancement reagents along with the ATPS components to improve ease-of-use of the ACE-LFA for these applications. We also plan to investigate and integrate other signal enhancement reactions with the ACE-LFA, particularly those that can occur at a physiological pH.

CONCLUSION

In summary, we have developed a new method to automate sequential reagent delivery on paper-based devices using ATPS separation and flow on paper. The timing of reagent delivery could be controlled by altering the initial composition of the ATPS. To our knowledge, the ACE-LFA is the first reported technology with the capability to automate biomarker concentration, capture, and signal enhancement in a single paper-based device, as well as the first reported automation of a nanozyme signal enhancement reaction. Thus, this work plays a significant role in the advancement of paper-based devices with improved functionalities. Furthermore, with a 10-fold or greater improvement in detection limit within 30 min, the ACE-LFA has the ability to rapidly identify pathogens at lower concentrations than were previously detectable with the conventional LFA, all while maintaining a low cost, involving minimal user interaction, and requiring no electricity or laboratory equipment. Therefore, our ACE-LFA technology has the potential to greatly improve the state of disease detection in resource-poor regions which would ultimately lead to more effective patient management, treatment, and outbreak prevention.

ASSOCIATED CONTENT

Supporting Information

The Supporting Information is available free of charge on the ACS Publications website.

ATPS compositions, synthesis of PtGNs, description of signal development video, quantification of signal development video, LFA results comparing PtGNPs to GNPs, LFA results with increased sample volume (PDF)

Video of signal development comparing conventional LFA and ACE-LFA (mp4)

AUTHOR INFORMATION

Corresponding Author

*Email: kamei@seas.ucla.edu

Notes

B.M. Wu and D.T. Kamei are founders of the company Phase Diagnostics that intends on commercializing this core technology. They have financial interests in Phase Diagnostics, which has licensed this intellectual property from the UC Regents.

ACKNOWLEDGMENTS

This work was supported by NSF grant 1707194.

REFERENCES

(1) Top 10 Causes of Death. *World Heal. Organ.* **2016**, Geneva, Switzerland.

(2) Gubala, V.; Harris, L. F.; Ricco, A. J.; Tan, M. X.; Williams, D. E. Point of Care Diagnostics: Status and Future. *Anal. Chem.* **2012**, *84*, 487–515. https://doi.org/10.1021/ac2030199.

(3) Cheung, S. F.; Cheng, S. K. L.; Kamei, D. T. Paper-Based Systems for Point-of-Care Biosensing. *J. Lab. Autom.* **2015**, *20*, 316–333. https://doi.org/10.1177/2211068215577197.

(4) Yager, P.; Domingo, G. J.; Gerdes, J. Point-of-Care Diagnostics for Global Health. *Annu. Rev. Biomed. Eng.* **2008**, *10*, 107–144. https://doi.org/10.1146/annurev.bioeng.10.061807.160524.

(5) Mashayekhi, F.; Chiu, R. Y. T.; Le, A. M.; Chao, F. C.; Wu, B. M.; Kamei, D. T. Enhancing the Lateral-Flow Immunoassay for Viral Detection Using an Aqueous Two-Phase Micellar System. *Anal. Bioanal. Chem.* **2010**, *398*, 2955–2961. https://doi.org/10.1007/s00216-010-4213-7.

(6) Jue, E.; Yamanishi, C. D.; Chiu, R. Y. T.; Wu, B. M.; Kamei, D. T. Using an Aqueous Two-Phase Polymer-Salt System to Rapidly Concentrate Viruses for Improving the Detection Limit of the Lateral-Flow Immunoassay. *Biotechnol. Bioeng.* **2014**, *111*, 2499–2507. https://doi.org/10.1002/bit.25316.

(7) Mashayekhi, F.; Le, A. M.; Nafisi, P. M.; Wu, B. M.; Kamei, D. T. Enhancing the Lateral-Flow Immunoassay for Detection of Proteins Using an Aqueous Two-Phase Micellar System. *Anal. Bioanal. Chem.* **2012**, *404*, 2057–2066. https://doi.org/10.1007/s00216-012-6278-y.

(8) Chiu, R. Y. T.; Nguyen, P. T.; Wang, J.; Jue, E.; Wu, B. M.; Kamei, D. T. Dextran-Coated Gold Nanoprobes for the Concentration and Detection of Protein Biomarkers. *Ann. Biomed. Eng.* **2014**, *42*, 2322–2332. https://doi.org/10.1007/s10439-014-1043-3.

(9) Chiu, R. Y. T.; Jue, E.; Yip, A. T.; Berg, A. R.; Wang, S. J.; Kivnick, A. R.; Nguyen, P. T.; Kamei, D. T. Simultaneous Concentration and Detection of Biomarkers on Paper. *Lab Chip* **2014**, *14*, 3021–30288. https://doi.org/10.1039/c4lc00532e.

(10) Pereira, D. Y.; Chiu, R. Y. T.; Zhang, S. C. L.; Wu, B. M.; Kamei, D. T. Single-Step, Paper-Based Concentration and Detection of a Malaria Biomarker. *Anal. Chim. Acta* **2015**, *882*, 83–89. https://doi.org/10.1016/j.aca.2015.04.040.

(11) Cho, J. H.; Paek, E. H.; Cho, I. I. H.; Paek, S. H. An Enzyme Immunoanalytical System Based on Sequential Cross-Flow Chromatography. *Anal. Chem.* **2005**, *77*, 4091–4097. https://doi.org/10.1021/ac048270d.

(12) Cho, I.-H.; Bhunia, A.; Irudayaraj, J. Rapid Pathogen Detection by Lateral-Flow Immunochromatographic Assay with Gold Nanoparticle-Assisted Enzyme Signal Amplification. *Int. J. Food Microbiol.* **2015**, *206*, 60–66. https://doi.org/10.1016/j.ijfoodmicro.2015.04.032.

(13) Fu, E.; Kauffman, P.; Lutz, B.; Yager, P. Chemical Signal Amplification in Two-Dimensional Paper Networks. *Sensors Actuators, B Chem.* **2010**, *149*, 325–328. https://doi.org/10.1016/j.snb.2010.06.024.

(14) Fu, E.; Liang, T.; Houghtaling, J.; Ramachandran, S.; Ramsey, S. a.; Lutz, B.; Yager, P. Enhanced Sensitivity of Lateral Flow Tests Using a Two-Dimensional Paper Network Format. *Anal. Chem.* **2011**, *83*, 7941–7946. https://doi.org/10.1021/ac201950g.

(15) Lutz, B. R.; Trinh, P.; Ball, C.; Fu, E.; Yager, P. Two-Dimensional Paper Networks: Programmable Fluidic Disconnects for Multi-Step Processes in Shaped Paper. *Lab Chip* **2011**, *11*, 4274–4278. https://doi.org/10.1039/c1lc20758j.

(16) Fu, E.; Liang, T.; Spicar-Mihalic, P.; Houghtaling, J.; Ramachandran, S.; Yager, P. Two-Dimensional Paper Network Format That Enables Simple Multistep Assays for Use in Low-Resource Settings in the Context of Malaria Antigen Detection. *Anal. Chem.* **2012**, *84*, 4574–4579. https://doi.org/10.1021/ac300689s.

(17) Park, J.; Shin, J. H.; Park, J. K. Pressed Paper-Based Dipstick for Detection of Foodborne Pathogens with Multistep Reactions. *Anal. Chem.* **2016**, *88*, 3781–3788. https://doi.org/10.1021/acs.analchem.5b04743.

(18) Toley, B. J.; McKenzie, B.; Liang, T.; Buser, J. R.; Yager, P.; Fu, E. Tunable-Delay Shunts for Paper Microfluidic Devices. *Anal. Chem.* **2013**, *85*, 11545–11552. https://doi.org/10.1021/ac4030939.

(19) Gerbers, R.; Foellscher, W.; Chen, H.; Anagnostopoulos, C.; Faghri, M. A New Paper-Based Platform Technology for Point-of-Care Diagnostics. *Lab Chip* **2014**, *14*, 4042–4049. https://doi.org/10.1039/C4LC00786G.

(20) Toley, B. J.; Wang, J. a.; Gupta, M.; Buser, J. R.; Lafleur, L. K.; Lutz, B. R.; Fu, E.; Yager, P. A Versatile Valving Toolkit for Automating Fluidic Operations in Paper Microfluidic Devices. *Lab Chip* **2015**, *15*, 1432–1444. https://doi.org/10.1039/C4LC01155D.

(21) Phillips, E. A.; Shen, R.; Zhao, S.; Linnes, J. C. Thermally Actuated Wax Valves for Paper-Fluidic Diagnostics. *Lab Chip* **2016**, *16*, 4230–4236. https://doi.org/10.1039/C6LC00945J.

(22) Kong, T.; Flanigan, S.; Weinstein, M.; Kalwa, U.; Legner, C.; Pandey, S. A Fast, Reconfigurable Flow Switch for Paper Microfluidics Based on Selective Wetting of Folded Paper Actuator Strips. *Lab Chip* **2017**, *17*, 3621–3633. https://doi.org/10.1039/C7LC00620A.

(23) Lutz, B.; Liang, T.; Fu, E.; Ramachandran, S.; Kauffman, P.;

Yager, P. Dissolvable Fluidic Time Delays for Programming Multi-Step Assays in Instrument-Free Paper Diagnostics. *Lab Chip* **2013**, *13*, 2840–2847. https://doi.org/10.1039/c3lc50178g.

(24) Jahanshahi-Anbuhi, S.; Kannan, B.; Pennings, K.; Ali, M. M.; Leung, V.; Giang, K.; Wang, T.; White, D.; Li, Y.; Pelton, R. H.; Brennan, J. D.; Filipe, C. D. M. Automating Multi-Step Paper-Based Assays Using Integrated Layering of Reagents. *Lab Chip* **2017**, *17*, 943–950. https://doi.org/10.1039/C6LC01485B.

(25) Fu, E.; Downs, C. Progress in the Development and Integration of Fluid Flow Control Tools in Paper Microfluidics. *Lab Chip* **2017**, *17*, 614–628. https://doi.org/10.1039/C6LC01451H.

(26) Gao, Z.; Ye, H.; Tang, D.; Tao, J.; Habibi, S.; Minerick, A.; Tang, D.; Xia, X. Platinum-Decorated Gold Nanoparticles with Dual Functionalities for Ultrasensitive Colorimetric in Vitro Diagnostics. *Nano Lett.* **2017**, *17*, 5572–5579. https://doi.org/10.1021/acs.nanolett.7b02385.

(27) Asenjo, J. A.; Andrews, B. A. Aqueous Two-Phase Systems for Protein Separation: Phase Separation and Applications. *J. Chromatogr. A* **2012**, *1238*, 1–10. https://doi.org/10.1016/j.chroma.2012.03.049.

(28) Oh, K. W.; Lee, K.; Ahn, B.; Furlani, E. P. Design of Pressure-Driven Microfluidic Networks Using Electric Circuit Analogy. *Lab Chip* **2012**, *12*, 515–545. https://doi.org/10.1039/c2lc20799k.

(29) Mosley, G. L.; Pereira, D. Y.; Han, Y.; Lee, S. Y.; Wu, C. M.; Wu, B. M.; Kamei, D. T. Improved Lateral-Flow Immunoassays for Chlamydia and Immunoglobulin M by Sequential Rehydration of Two-Phase System Components within a Paper-Based Diagnostic. *Microchim. Acta* **2017**, *184*, 4055–4064. https://doi.org/10.1007/s00604-017-2434-6.

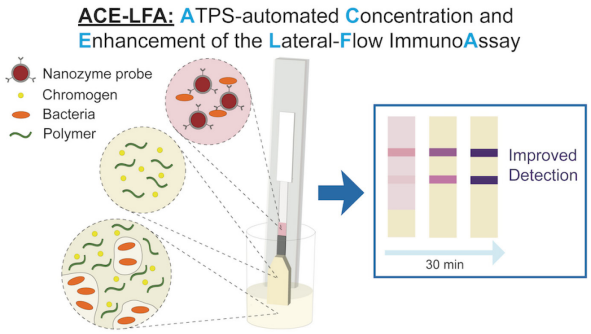
ACE-LFA: ATPS-automated Concentration and
Enhancement of the Lateral-Flow ImmunoAssay
Nanozyme probe
Chromogen
Bacteria
Polymer
Improved
Detection
30 min